

Modelling the dynamics of fermentation and respiratory processes in a groundwater plume of phenolic contaminants interpreted from laboratory- to field-scale

**IAN A. WATSON^{1,2}, SASCHA E. OSWALD^{1,3}, STEVEN A. BANWART^{1*},
ROGER S. CROUCH¹ AND STEVEN F. THORNTON¹**

1. Groundwater Protection and Restoration Group, Department of Civil and Structural Engineering, University of Sheffield, Mappin Street, Sheffield S1 3JD, United Kingdom.

2. Present address: The Coal Authority, 200 Lichfield Lane, Mansfield, Nottinghamshire NG18 4RG, United Kingdom

3. Department Hydrogeology (HDG), UFZ Centre for Environmental Research Leipzig-Halle GmbH, Theodor-Lieser-Str. 4, 06120 Halle, Germany

* Corresponding author: telephone: +44/0 114 222 5743 fax: +44/0 114 222 5700 e-mail: s.a.banwart@sheffield.ac.uk

7 pages

2 figures

3 tables

Simulation of Source Area

The simulated source is estimated from mass balance by summation of the undegraded phenol, the biodegradation intermediates and end-products within the plume. Forensic analysis of concentration profiles for phenol, biodegradation intermediates and end-products in BH59 and BH60 allows the source term to be estimated at times of approximately 15 years and 35 years before present. The source zone is treated as a 20m vertical line source which, for each source species, is described as discrete segments of

fixed source strength. Because of the relatively small decrease in total phenols mass within the plume, the vertical distribution of source strength is strongly constrained by the concentration profile at the two MLS locations downgradient of the source zone.

Representation of Flow and Permeability Field

The plume is plunging (Fig. 1) due to recharge, a water supply well pumping at 80m depth 2km to the west, a dip of bedding, and possibly density effects (see (1) for a site description). Trial simulations demonstrated that the amount of TEAs, e.g. $O_2(aq)$, reaching the plume from recharge at the water table was negligible. The computational effort was therefore focused on minimising numerical dispersion rather than simulating recharge sustaining a negligible mass flux of aqueous oxidants to the aquifer. Therefore the grid was aligned parallel to the plume, and no-flow boundaries were used at the top and bottom of the model domain (cf. 2). It is assumed the flow field has been steady throughout the 47 year simulation period. The unpublished horizontal transect data described above, at the locations of BH59 and BH60, confirm that the vertical profiles do not vary significantly laterally across the plume flowpath. This indicates strongly that these field observations are representative of hydrochemical signatures occurring at two locations along a single flowline downgradient of the source. The parameter values for physical flow and transport are given in Table 4.

To examine the effect of a spatially variable flow field on the interpretation of the reactive system, a representative heterogeneous 2-D permeability field including vertical anisotropy was created. Horizontal hydraulic conductivity data from the consolidated Triassic sandstone aquifer at the field site shows a range of 0.2 to 1.3 m/day (1).

Stochastic parameters (see Table S.1) were therefore chosen to yield a permeability range of ca. one order of magnitude around the mean, which is a relatively mild degree of heterogeneity comparable to conditions at the Borden site. The resulting flow field has a horizontal velocity component, q_x which is approximately 20 times larger than the vertical component q_z .

This model was used with a homogeneous flow field as a baseline case to compare the plume mass balance with the spatially-variable flow field scenario. Sensitivity analysis of the model parameters is presented elsewhere (3). Non-reactive models were also run to assess the relative importance of reactive processes that give rise to the observed biodegradation intermediates and products, given the small mass fraction of phenol which has degraded in the plume.

The Influence of Physical Flow and Transport

A comparison of homogeneous and heterogeneous flow-field simulations is shown in Fig. S.1. These are similar except for some increased fingering and a slightly broader, more dispersed plume in the heterogeneous flow-field. This strongly indicates that the distribution of chemical species in the plume is primarily controlled by the spatially and temporally variable concentration field in the source area and biogeochemical reactions within the plume, rather than spatial variability of the flow-field. A further control is the spatial variation in biodegradation rates through the plume. This arises from the variation in phenol concentration between the plume core and the plume fringe, and the resulting relative inhibition of biodegradation due to phenol substrate toxicity.

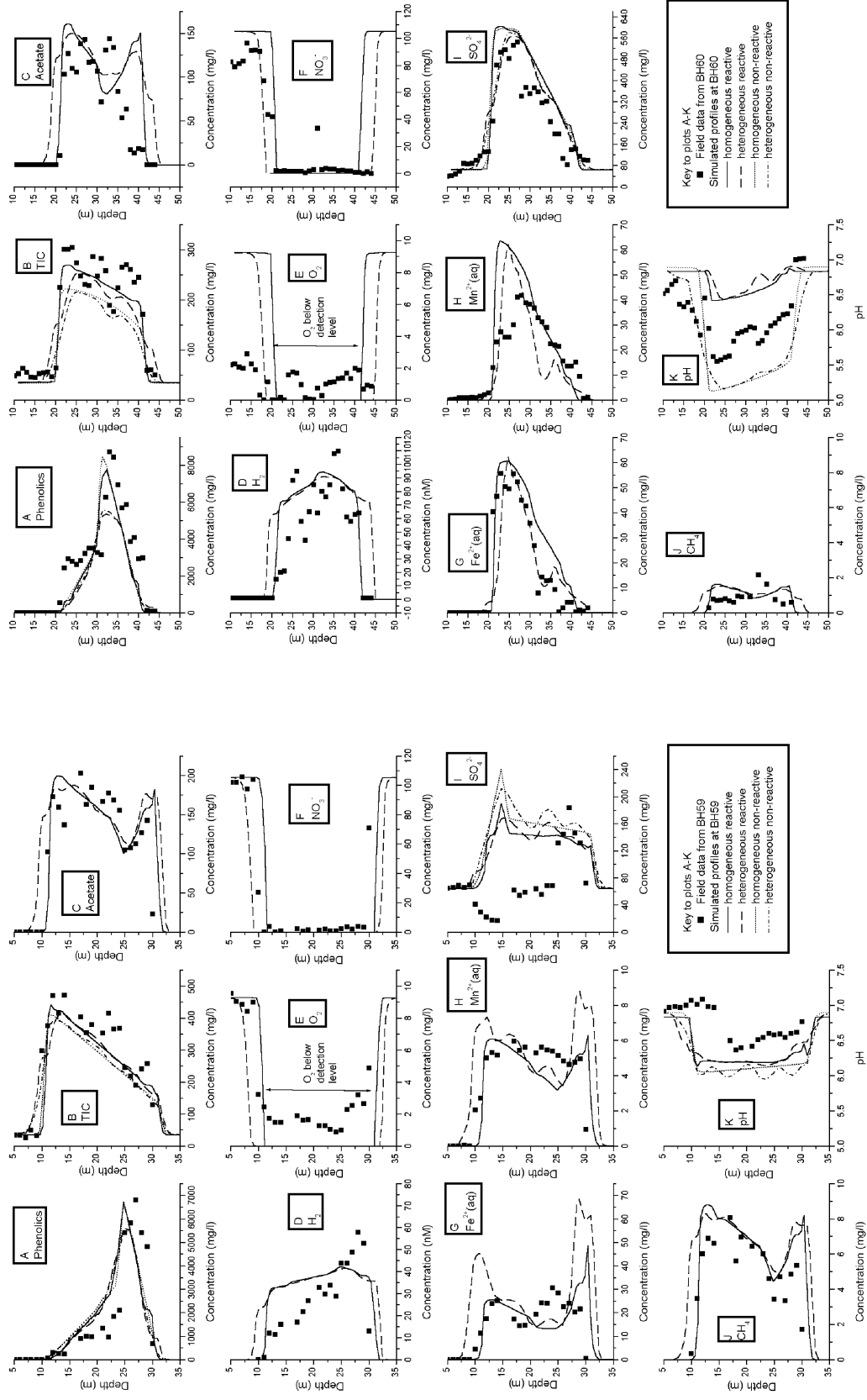


Figure S.1. BH59 concentration profiles (x=130m, left), BH60 concentration profiles (x=350m, right), showing one set of observed data, and simulation results from both, homogeneous and heterogeneous flow models, with both reactive and non-reactive cases after 47 years.

The simulated O_2 and NO_3^- profiles for a heterogeneous flow field clearly imply that the plume is wider in the vertical dimension. This is due to the increased apparent transverse dispersion which leads to a higher rate of dispersive mixing and mass turnover of phenol at the plume fringe, via these TEAPs. With respect to the mass balance (Table 6) the heterogeneous flow field simulation results in a significantly higher (~20%) phenol degradation rate.

Change in Sulphate Profile with Time in Borehole BH59

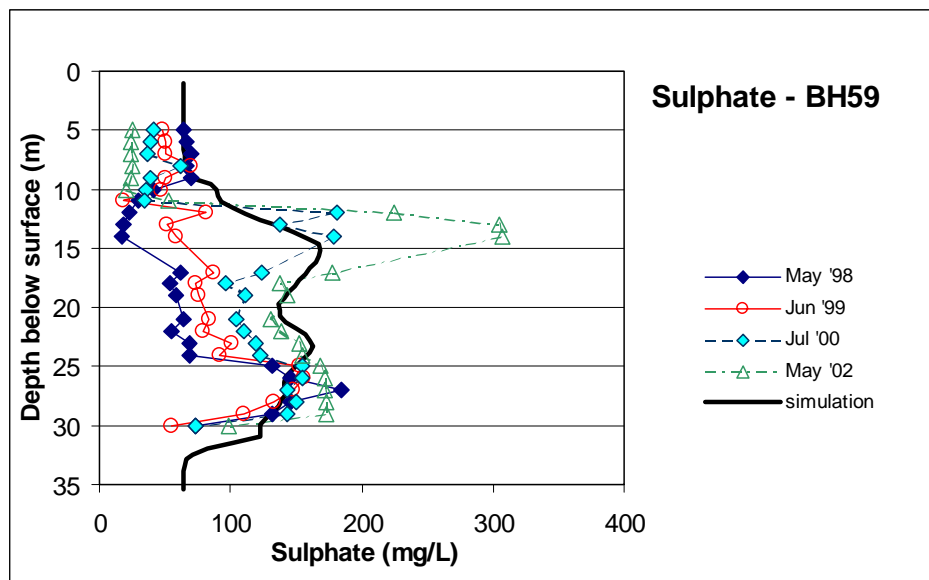


Figure S.2. Sulphate profile at BH59 comparing simulation results at 50 years with field data collected over 4 years.

Sulphate profiles in BH59 were the only the only vertical profile in either BH59 or BH60 to show significant variation over the four year sampling period. Although a rising trend is clear over these four years, this was not felt to be significant over the 47 year plume life, so the simulation did not intend to capture this short term trend. The simulated profile echoes the form of the later two field data sets much more strongly than the earlier two field data sets.

Physical Properties and Thermodynamic Data

Table S.1. Physical parameters used for reactive transport simulations Parameter	Value
Effective porosity (-)	0.125 ^a
Hydraulic conductivity, K_x (m/s)	8.4×10^{-6} ^a
Hydraulic gradient (-)	4.2×10^{-3} ^a
Longitudinal dispersivity (m)	1.0 ^a
Vertical transverse dispersivity (m)	4.0×10^{-4} ^a
Final solution time (year)	47 ^a
Max time step size (year)	0.05 ^b
Domain size, length X (m)	750 ^a
Domain size, height Z (m)	40 ^a
Max elements in X	256 ^c
Max elements in Z	64 ^c
Parameters for heterogeneous anisotropic 2D flow field	
Correlation length in x (m)	10
Correlation length in z (m)	1
Variance applied to K_x	0.1
Anisotropy K_x / K_z	100 ^d

Notes:

a – same as in Mayer *et al* (2)

b - adaptive time stepping used up to this maximum dt

c - local adaptive remeshing was applied up to the most refined multigrid level 6 which has $2^6 = 64$ times more elements than level 0.

d – a similar anisotropy value was estimated in field scale trial simulations considering head gradient vector and plume travel direction.

Table S.2. Thermodynamic equilibrium data for reactions included in simulation.

Aqueous Complexation Reaction	Log K
$H_2O = H^+ + OH^-$	-13.998
$H_2CO_3 = H^+ + HCO_3^-$	-6.351
$HCO_3^- = H^+ + CO_3^{2-}$	-10.330
Mineral Dissolution/Precipitation	
$FeS + H^+ = Fe^{2+} + HS^-$	-4.648
Surface Complexation Reaction	
$>FeOH_{(w)} + H^+ = >FeOH_2^+_{(w)}$	7.29
$>FeOH_{(w)} = >FeO^-_{(w)} + H^+$	-8.93
$>FeOH_{(w)} + Fe^{2+} = >FeOFe^+_{(w)} + H^+$	-2.98
$>FeOH_{(w)} + Fe^{2+} + H_2O = >FeOFeOH_{(w)} + 2H^+$	-11.55
$>FeOH_{(w)} + Mn^{2+} = >FeOMn^+_{(w)} + H^+$	-3.50

Thermodynamic data used is taken from WATEQ4F database as used in PHREEQC2 (4).

Activity coefficients were calculated using the Davies equation. Temperature corrections were not applied in this simulation.

Table S.3. Monod and inhibition parameters for simulation of kinetic redox reactions as in Table 1, K_M and K_I parameters as in eq. (1)

	Substrate, S	TEA	Half saturation constants		Inhibition terms		
			$K_{M,S}$ [mol/l]	$K_{M,TEA}$ [mol/l]	$K_I O_2$ [mol/l]	$K_I NO_3$ [mol/l]	$K_I C_6H_6O$ [mol/l]
1	C_6H_6O	O_2	1.1×10^{-4a}	3.1×10^{-6a}	-	-	-
2	C_6H_6O	NO_3^-	1.1×10^{-4a}	8.1×10^{-6a}	6.2×10^{-6a}	-	-
3	C_6H_6O	-	1.1×10^{-4b}	-	3.1×10^{-5a}	1.6×10^{-5a}	6.0×10^{-2c}
4	C_6H_6O	-	1.1×10^{-4b}	-	3.1×10^{-5a}	1.6×10^{-5a}	6.0×10^{-2c}
5	H_2	$Mn(IV)_{(s)}$	5.0×10^{-7b}	-	3.1×10^{-5a}	1.6×10^{-5a}	4.0×10^{-2c}
6	H_2	$Fe(III)_{(s)}$	5.0×10^{-7b}	-	3.1×10^{-5a}	1.6×10^{-5a}	4.0×10^{-2c}
7	H_2	SO_4^{2-}	1.0×10^{-6b}	1.6×10^{-3d}	3.1×10^{-5a}	1.6×10^{-5a}	4.0×10^{-2c}
8	H_2	TIC	5.0×10^{-6b}	-	3.1×10^{-5a}	1.6×10^{-5a}	4.0×10^{-2c}

Notes: reaction numbers as in Table 1

a – same as in Mayer *et al* (2)

b – same as in Watson *et al* (5)

c – calibrated, value in (2) of $K_I C_6H_6O = 6.4 \times 10^{-3}$

d – calibrated, value in (2) of $K_{M,SO4} = 1.6 \times 10^{-3}$

References

- (1) Williams, G. M.; Pickup, R. W.; Thornton, S. F.; Lerner, D. N.; Mallinson, H. E. H.; Moore, Y.; White, C. Biogeochemical characterisation of a coal tar distillate plume. *Journal of Contaminant Hydrology* **2001**, *53*, 175-197.
- (2) Mayer, K. U.; Benner, S. G.; Frind, E. O.; Thornton, S. F.; Lerner, D. N. Reactive transport modeling of processes controlling the distribution and natural attenuation of phenolic compounds in a deep sandstone aquifer. *Journal of Contaminant Hydrology* **2001**, *53*, 341-368.
- (3) Watson, I. A.; S. E.; Crouch, R. S.; Bastian, P.; Oswald, S. E. Advantages of using locally adaptive remeshing and parallel processing in modelling biodegradation in groundwater. *Advances in Water Resources* **2005**, in press.
- (4) Parkhurst, D. L.; Appelo, C. A. J. "User's guide to PHREEQC (version 2)- A computer program for speciation, batch-reaction, one-dimensional transport, and inverse geochemical calculations.," USGS, 1999.
- (5) Watson, I. A.; Oswald, S. E.; Mayer, K. U.; Wu, Y. X.; Banwart, S. A. Modeling kinetic processes controlling hydrogen and acetate concentrations in an aquifer-derived microcosm. *Environmental Science & Technology* **2003**, *37*, 3910-3919.